ACS OMEGA

Article

Cite This: ACS Omega 2019, 4, 1095−1102

http://pubs.acs.org/journal/acsodf

Effect of Liquid Crystalline Texture of Mesophase Pitches on the Structure and Property of Large-Diameter Carbon Fibers

Guanming Yuan,*[,†] Baoliu Li,[‡] Xuanke Li,*[,†,‡] Zhijun Dong,[†] Wanjing Hu,[†] Aidan Westwood,[§] Ye Cong,[†] and Jiang Zhang[†]

[†]The State Key Laboratory of Refractories and Metallurgy, Wuhan University of Science and Technology, Wuhan 430081, China

[‡]The Research Center for Advanced Carbon Materials, Hunan University, Changsha 410082, China

[§]School of Chemical and Process Engineering, University of Leeds, Leeds LS2 9JT, United Kingdom

ABSTRACT: Two types of carbon fibers with a large diameter of ∼22 μm, derived from unstirred and vigorously stirred mesophase pitch melts with different liquid crystalline mesophase textures, were prepared by melt-spinning, stabilization, carbonization, and graphitization treatments. The morphology, microstructure, and physical properties of the carbon fibers derived from the two kinds of mesophase precursors after various processes were characterized in detail. The results show that the optical texture (i.e., size and orientation) of the liquid crystalline mesophase in the molten pitch is obviously modified by thermomechanical stirring treatment, which has a significant effect on the texture of as-spun pitch fibers, and finally dominates the microstructure and physical properties of the resulting carbon and graphite fibers. These large-diameter fibers expectedly maintain their morphological and structural integrity and effectively avoid shrinkage cracking during subsequent high-temperature heat treatment processes, in contrast to those derived from the unstirred pitch. This is due to the smaller crystallite sizes and lower orientation of graphene layers in the former. The tensile strength and axial electrical resistivity of the 3000 °C-graphitized large fibers derived from the unstirred pitch are about 1.8 GPa and 1.18 μΩ m, respectively. In contrast, upon melt stirring treatment of the pitch before spinning, the resulting large-diameter graphite fibers possess the corresponding values of 1.3 GPa and 1.86 μΩ m. Despite the acceptable decrease of mechanical properties and axial electrical and thermal conduction performance, the latter possesses relatively high mechanical stability (i.e., low strength deviation) and ideal morphological and structural integrity, which is beneficial for the wide applications in composites.

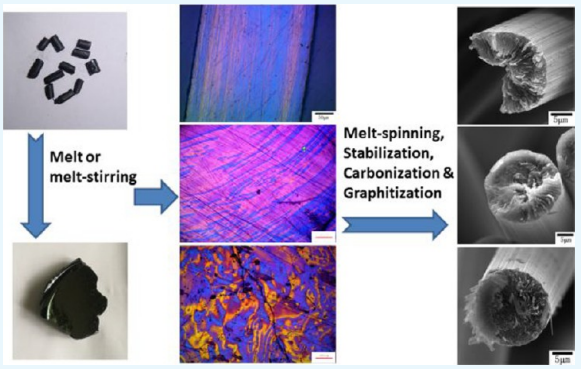

1. INTRODUCTION

Mesophase pitch-based carbon fibers have the potential to attain moduli values up to the theoretical modulus of graphite, 1000 GPa, merely by high-temperature heat treatment and have higher axial electrical (as low as 1.1 μΩ m) and thermal conductivities (exceeding 1000 W/m K; cf. carbon fibers derived from polyacrylonitrile or rayon).[1−3] All these overwhelming factors make them particularly suitable for many critical aviation and aerospace applications. It is known that the macroscopic properties of carbon fibers are determined by their microstructure and there is great potential to tailor their structure during the liquid crystalline phase of the synthesis process[4] because the structure and properties of carbon (and hence graphite) fibers have a close relationship to those of their pitch fiber precursors.[1,5] For example, the smaller the diameter of a pitch fiber, the higher the tensile strength of the resulting carbon fiber, and the performance of the carbon fiber from the pitch fiber with a concentric "onion" structure is better than that from a radial structure. To obtain such promising fibers, it is necessary to modify the structure and property of the pitch precursor, change the shape and structure of the spinneret, and adjust the spinning conditions (e.g., extrude temperatures).[1,5−7] However, controllably preparing such onion-textured carbon fibers is currently still very difficult.

It is well demonstrated that radial-textured round carbon fibers are prone to split-forming an open wedge-shaped "Pac-man" cross-sectional configuration during a high-temperature heat treatment processes.[7−10] This will undoubtedly affect their final physical properties (e.g., variable strength distribution) and limit their potential application for high volume fraction packing, for example, in composites. Many studies have been performed to control or eliminate the crack splitting texture of carbon fibers to achieve an ideal structure and good physical (mechanical or thermal conduction) performance. For instance, Hamada et al. successfully disrupted the radial texture by the placement of a mixer directly above the spinning nozzle to obtain textures from random to quasi-onion.[11] Mochida et al. employed noncircular spinning nozzles and designed the

Received: November 15, 2018
Accepted: January 2, 2019
Published: January 14, 2019

DOI: 10.1021/acsomega.8b03189
ACS Omega 2019, 4, 1095−1102

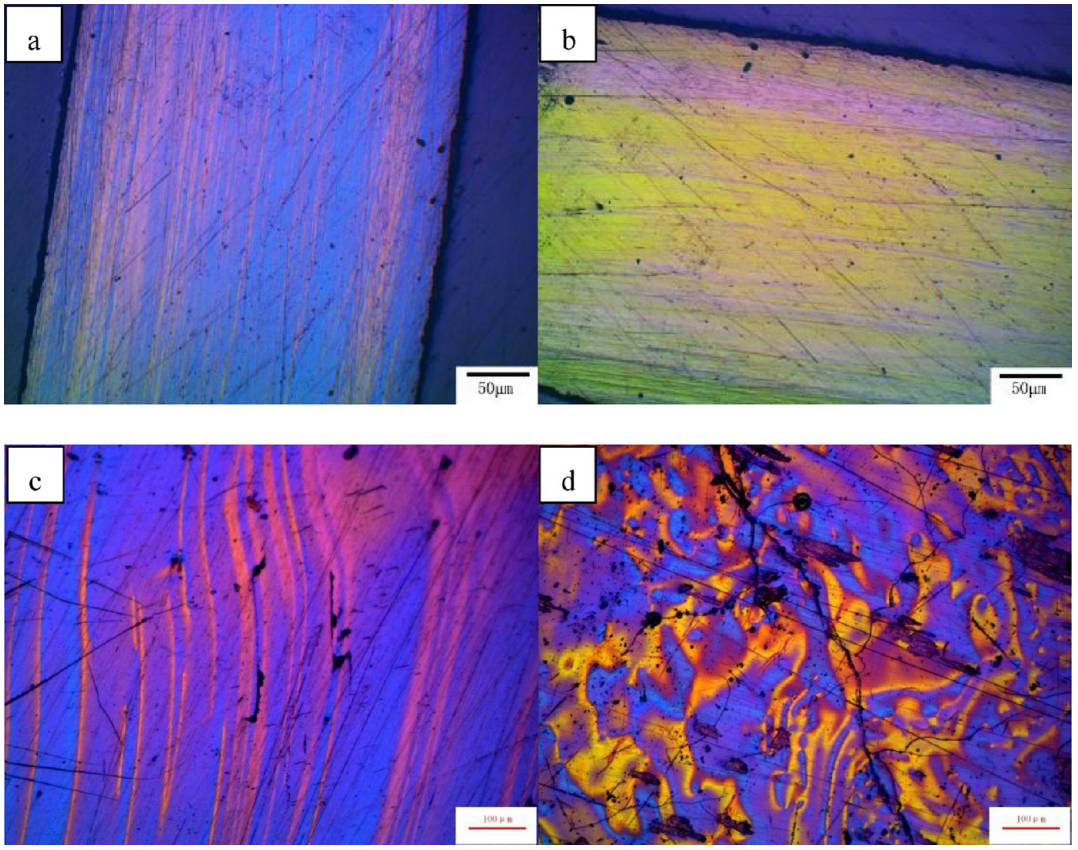

Figure 1. Typical PLM photographs of the (a, b) as-received, (c) melted, and (d) melt-stirred mesophase pitches.

geometries of the spinnerets and aspects of the capillary to control the transversal texture of round-shaped carbon fibers.[9,12] Matsumoto et al. used several types of nozzle and a fine-mesh filter to eliminate crack generation along the fiber axis.[13] Yao et al. adjusted the various components of the mesophase pitch by blending some isotropic pitches[14] and adopted a mesh filter above the spinneret[15] to tailor the microstructure and physical properties of carbon fibers. In addition, some nano- or microsized carbon materials[16,17] (e.g., carbon nanotubes, carbon black, and graphene) have been added into the mesophase pitch to modify the structure and property of the resultant carbon fibers.

In the previous research, agitating the pitch melt directly above the spinning nozzle requires very high seal performance for pumping the melt out of the nozzle and may be unfavorable for continuous or industrial spinning and homogeneous fiber texture owing to the incidence of some bubbles and the instantaneous inhomogeneity of the pitch melt, which will undoubtedly affect the final properties of carbon fibers. In this work, it is very simple and effective to modify the rheological structure (i.e., the microdomain size, arrangement, and orientation of the liquid crystalline mesophase) of the pitch melt by vigorous thermomechanical stirring treatment on a bulk mesophase pitch with 100% optically anisotropic content (that easily formed radial-cracked carbon fibers in previous work, especially large-diameter fibers[18]) before melt-spinning. Furthermore, this work provides a complete study to elucidate the effect of the liquid crystalline mesophase texture on the microstructure and properties of the resulting carbon fibers and, in particular, those with large diameters. Large-diameter carbon fibers (Φ ~22 μm) prepared from the unstirred and stirred pitches are selected as a model to confirm the experimental effect because large-diameter carbon fibers are more prone to split during heat treatment processes.

2. RESULTS AND DISCUSSION

2.1. Optical Texture of the Pitch and Its Derivatives.

The polarized-light micrographs of the as-received, melted and melt-stirred mesophase pitches are shown in Figure 1. It can be seen that the as-received pitch, shown in Figure 1a, b, possesses a streamline "fibrous" texture with high orientation (i.e., an orderly liquid crystalline phase) visible via orthogonal observation by rotating the object stage of the PLM. Following melting and melt-stirred treatments at 320 °C as shown in Figure 1c, d, respectively, the optical texture of the melting pitch is nearly maintained, and the conformation and orientation of the macromolecules in the melt-stirred pitch are disrupted to become partially disordered or turbulent (severely deformed),[19,20] depending upon the degree of stirring. Nevertheless, the optically anisotropic content of the two types of pitches is not changed, and the anisotropy and size of the polydomain structure of the liquid crystalline mesophase reduced, as expected, upon intensive stirring and shearing. Figure 2 shows typical PLM photographs of the as-spun pitch fibers from as-received and melt-stirred mesophase pitches. It can be clearly found that there is an obvious difference in the distribution and size of isochromatic color regions (which are in close relation to the orientation and size of the microcrystalline domains within the resulting carbon fibers) in the transverse cross sections of the respective as-spun pitch fibers. That is to say the arrangement, orientation, and distribution of the liquid crystalline mesophase in the as-spun

DOI: 10.1021/acsomega.8b03189
ACS Omega 2019, 4, 1095−1102

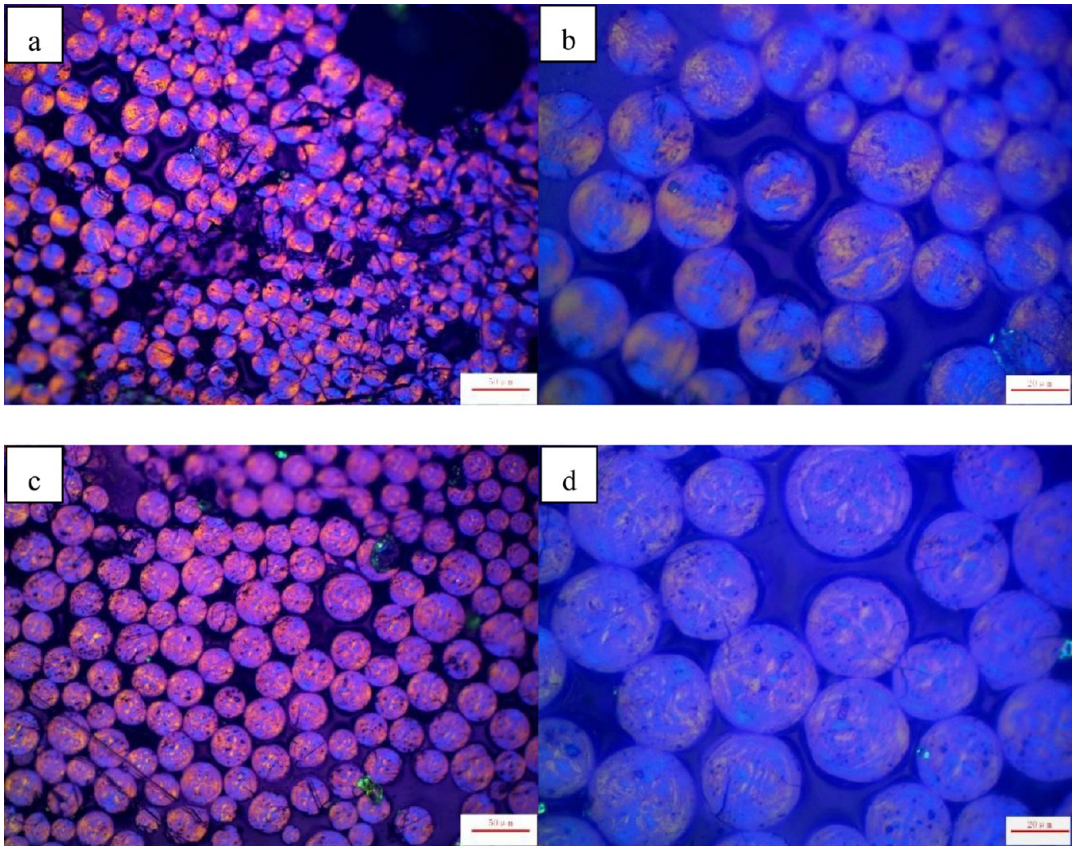

Figure 2. Typical PLM photographs of the as-spun pitch fibers from the (a, b) as-received and (c, d) melt-stirred mesophase pitches at various magnifications.

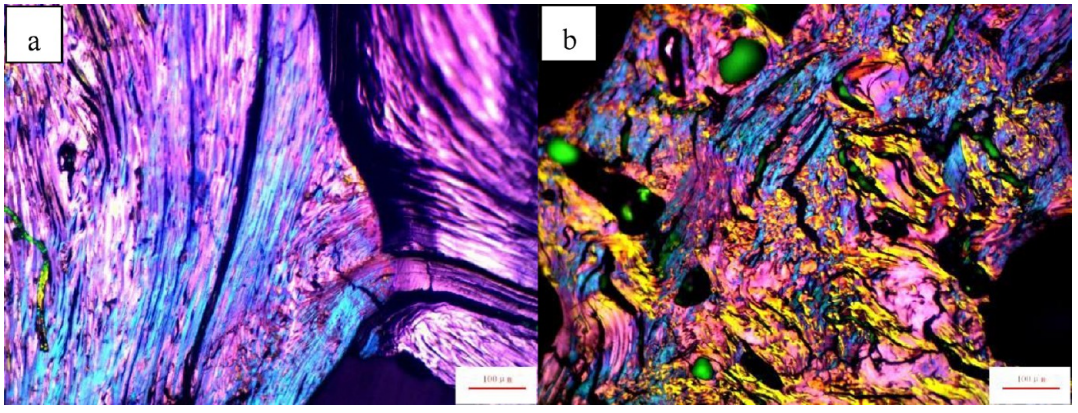

Figure 3. Typical PLM photographs of 900 °C-carbonized coke derived from the (a) as-received and (b) melt-stirred mesophase pitches.

fibers are disturbed by changing the rheological texture of the pitch precursor. Vigorous melt-stirring significantly homogenizes the initial anisotropic texture of the mesophase pitch and its derivative pitch fibers. As a necessary supplement, the typical PLM photographs of 900 °C-carbonized coke derived from the as-received and melt-stirred mesophase pitches are shown in Figure 3, which further demonstrate the two clearly different microstructures varying from a well-oriented texture to a supramosaic texture owing to the textural variety of mesophase pitches.

2.2. Morphology and Microstructures of the Derivative Carbon Fibers. Figures 4 and 5 show SEM images of the typical transverse cross sections of these carbon fibers heat-treated at various temperatures. The great majority of carbonized and graphitized fibers derived from the unstirred pitch exhibit radial open cracks as shown in Figure 4a–c, which show a typical "Pac-man" splitting texture. The carbon layers in the transverse cross section of large fibers radiate from the center to the surface like spokes in a wheel as shown in Figure 5a–c, in a similar fashion to the well-known K-1100 graphite fibers.[21] The highly preferred orientation of carbon layers running along the axial direction of the fiber is clearly observed in Figure 5b, c. The larger the diameter of the pitch fibers, the higher the degree of resultant carbon (graphite) fiber splitting in terms of both crack volume in the fiber bundle and crack angle of the single fiber.[22] The degree of splitting (opening angle) of large-diameter carbon fibers is obviously aggravated with an increase of heat treatment temperature

DOI: 10.1021/acsomega.8b03189
ACS Omega 2019, 4, 1095−1102

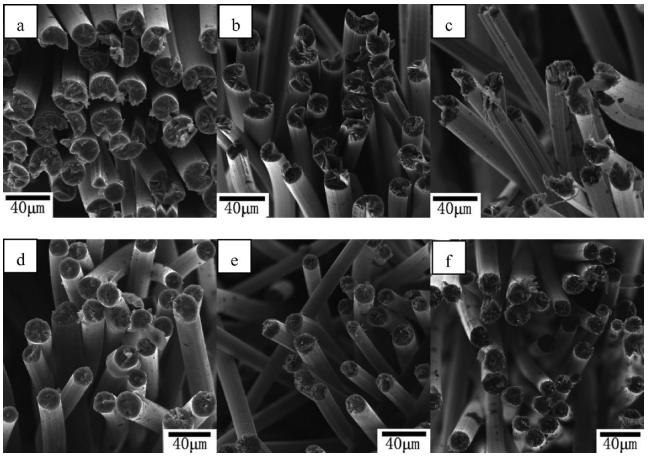

Figure 4. Typical SEM images of carbon fibers derived from the (a–c) unstirred and (d–f) stirred pitches after heat treatment at (a, d) 1000, (b, e) 2000, and (c, f) 3000 °C.

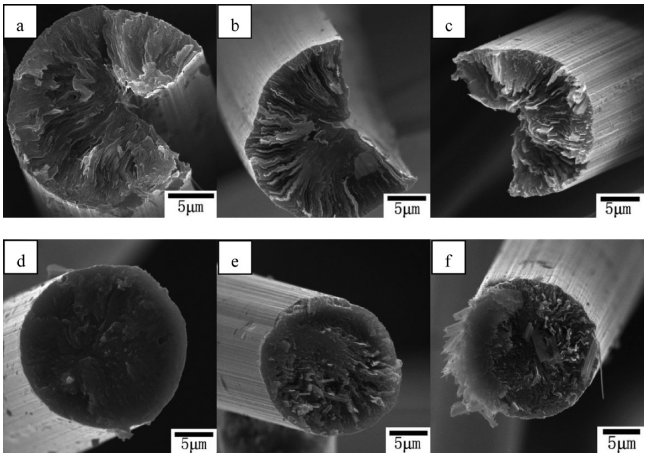

Figure 5. Typical SEM images of the magnified transverse sections of carbon fibers derived from the (a–c) unstirred and (d–f) stirred pitches after heat treatment at (a, d) 1000, (b, e) 2000, (c, f) 3000 °C.

(HTT). This is caused by internal stresses within such highly anisotropic materials because of the directional growth and preferred orientation of graphite microcrystallites in the fiber. That is to say, this is caused by the limited growth of graphite crystals in a fibrous narrow space. However, the splitting of the fibers enables the graphene layers to pack and register more perfectly, which will result in a higher modulus and electrical and thermal conductivity in the fiber axial direction.[23]

In contrast, no obvious cracks can be observed in the transverse sections of the carbon fibers derived from the stirred pitch as shown in Figures 4d–f and 5d–f. These carbon fibers exhibit typical random (or radial-folded, disturbed) textures and avoid shrinkage cracking during heat treatment processes, which is similar to the random structure of general-grade isotropic-pitch-based carbon fibers[5] and some small-diameter carbon fibers in previous work.[22] The bent, twisted, or wavy carbon layers and small microcrystal domains within these carbon fibers exhibiting a relatively low anisotropic degree (i.e. high isotropy) are inherited from the disordered and chaotic liquid crystalline texture in the pitch precursor, which may be disadvantageous to the free growth of microcrystal graphite or graphene layer and the closely related electrical and thermal transport properties, but can effectively prohibit the occurrence and propagation of fiber cracks because the shrinkage deformation and structural evolution of these fibers during heat treatment processing are relatively uniform so as to preserve morphological and structural integrity, which will improve their homogeneity in terms of both structure and properties.

As a supplementary experiment, the slightly melt-stirred mesophase pitch pretreated at about 320 °C for 1 h (the agitating speed was fixed) was used to prepare the 3000 °C-graphitized large fibers. A typical irregular-radial or radial-folded texture on the transverse sections of carbon fibers is clearly shown in Figure 6. These graphite fibers also possess a complete circular morphology instead of a "Pac-man" splitting texture.

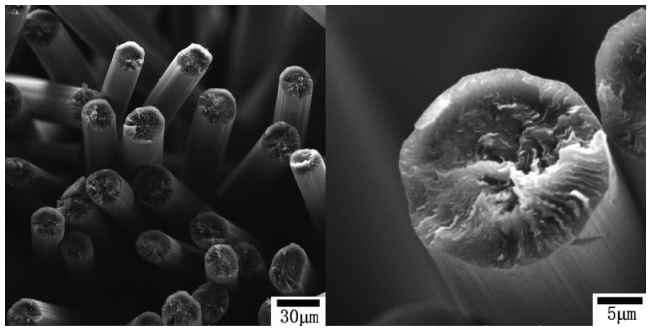

Figure 6. Typical SEM images of the transverse sections of the large carbon fibers derived from the slightly stirred pitch after heat treatment at 3000 °C.

It can be concluded that the microstructure of carbon fibers is inherited from the rheological structure of their mesophase pitch precursor, which can be varied to various extents by thermomechanical treatment before melt-spinning as shown in Figure 7. In mesophase pitch fiber manufacture, the molten

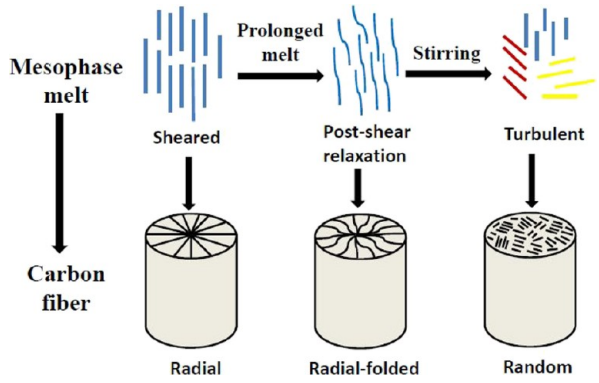

Figure 7. Schematic of the microstructure evolution from the mesophase pitch precursor to the transverse texture-controlled carbon fibers as the degree of melt-stirring increases.

liquid crystalline mesophase can be oriented within the spinneret by shear treatment during a melt-spinning process. In general, the shear forces involved result in a highly oriented structure, with the mesophase domains elongated into cylinders parallel to the fiber axis (circumferential fibers).[20,24] Provided that these shear forces are not sufficient to reorder the chaotic mesophase domains within the melt-stirred molten pitch (as shown in Figure 1d) in a transient extrusion process, various transversal textures, including radial, radial-folded, and

DOI: 10.1021/acsomega.8b03189
ACS Omega 2019, 4, 1095–1102

Table 1. Microcrystalline Parameters and Graphitization Degree (g) of the Two Types of Carbon Fibers Heat-Treated at Various Temperatures

	carbon fibers derived from the unstirred/stirred pitches				
HTT/°C	$2\theta_{(002)}$/°	$d_{(002)}$/nm	$L_{c(002)}$/nm[a]	$L_{a(100)}$/nm[a]	g/%[b]
1000	25.00/24.86	0.3561/0.3579	1.8/1.5	5.1/4.8	
1600	25.80/25.77	0.3451/0.3455	6.2/4.3	8.2/7.5	~0 for both
2000	26.17/26.07	0.3402/0.3415	19.3/14.4	15.8/13.8	44.2/29.1
2400	26.41/26.29	0.3372/0.3387	25.9/18.4	21.1/17.1	79.1/61.6
3000	26.45/26.40	0.3367/0.3373	27.8/20.9	42.8/18.7	84.9/77.9

[a] L values were calculated by the Scherrer equation $L = K\lambda/\beta\cos\theta$.[25] [b] g values were calculated by the expression $g = (0.3440 - d_{002}$ in nm$)/(0.3440 - 0.3354)$.[26]

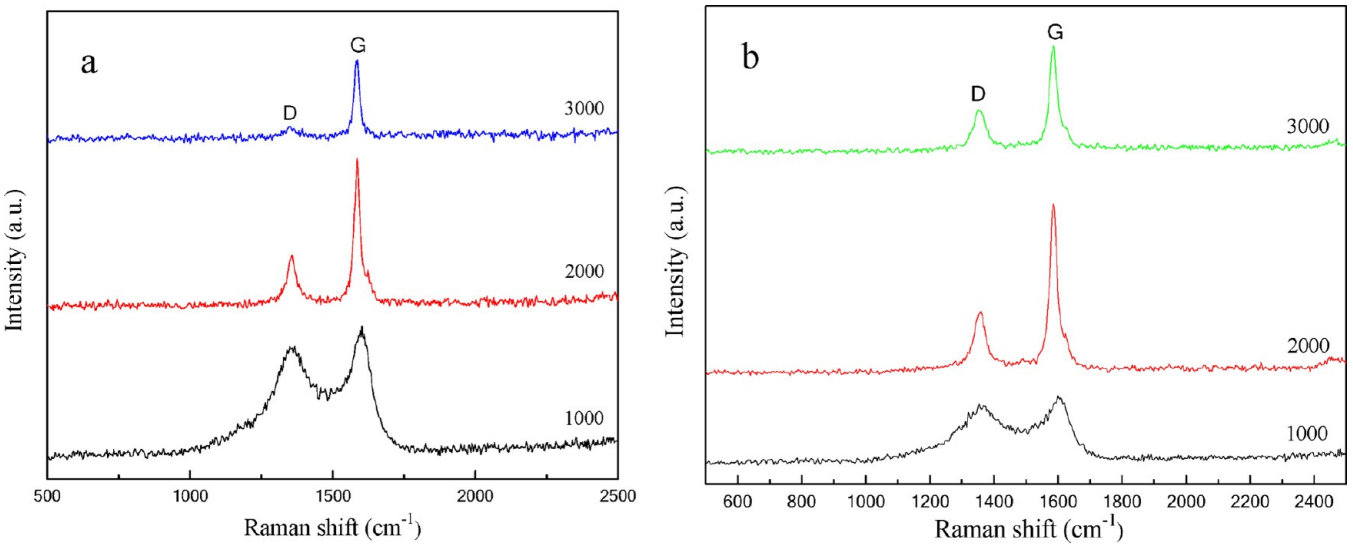

Figure 8. Raman spectra of the carbon fibers derived from the (a) unstirred and (b) stirred pitches after heat treatment at various temperatures, showing both D and G peaks.

random, and even quasi-onion, can be produced in the cross-sections of the resulting carbon fibers, which depends upon the chaotic degree of the liquid crystalline mesophase.

2.3. XRD and Raman Analyses of the Derivative Carbon Fibers. On the basis of XRD measurements, the microcrystalline parameters and graphitization degree (g) of the two types of carbon and graphite fibers heat-treated at various temperatures are listed in Table 1. With the increasing HTT, the interlayer spacing (d_{002}) of the carbon fibers obviously decreases, and the microcrystalline parameters (the crystallite thickness $L_{c(002)}$ and the crystallite length $L_{a(100)}$) and g values of the carbon fibers significantly increase. For the fiber samples heat-treated at the same temperature, the change of microcrystalline parameters of the carbon fibers derived from the unstirred pitch is more obvious (possessing larger crystal size and higher g value), which exhibits a good graphitizability.

It can be found that there is a small difference in the parameter values for the fiber samples carbonized at 1000 °C. However, the 3000 °C-graphitized large fibers derived from the unstirred pitch possess larger crystal size, higher g, and better crystalline orientation (strong and sharp (002) diffraction peak, not shown), whereas the carbon fibers derived from the stirred pitch exhibit smaller crystal size, lower g, and poor crystalline orientation. The growth of graphite crystallites within these fibers is severely inhibited owing to the severe curvature and wrinkling of carbon layers or domains in these fibers. The XRD analysis result is highly consistent with the SEM observation.

Figure 8 shows the typical first-order Raman spectra of the two types of carbon fibers heat-treated at various temperatures. The carbon fibers' D peak at about 1350 cm^{-1} and G peak at around 1580 cm^{-1} are both wide and intense, particularly at low HTTs. With the increase of HTT, the D and G peaks of the carbon fibers derived from the unstirred pitch as shown in Figure 5a become more sharp and symmetric, and both the intensity of the D peak and the I_D/I_G ratio of the fibers sharply decrease with the increase of HTT from 1000 to 3000 °C. This indicates a marked decrease in structural defects and disordered carbon concentrations in the final product and that the change from the turbostratic structure to the graphite structure has occurred through high-temperature heat treatment. It is interesting to note that the very weak D peak of the fibers graphitized at 3000 °C as shown in Figure 8a is similar to that of stress-annealed pyrolytic graphite,[27] which further reveals that a near-perfect crystal structure of graphite has formed in the graphite fibers. However, the decrease of intensity of the D peak and the I_D/I_G ratio of the carbon fibers derived from the stirred pitch as shown in Figure 8b is not as obvious as the former. The 3000 °C-graphitized fibers still exhibit a relatively strong D peak, which is closely associated with the disordered structure and small crystalline sizes inherited from the chaotic texture of the liquid crystalline mesophase pitch. This is in good agreement with the SEM and XRD measurements.

DOI: 10.1021/acsomega.8b03189
ACS Omega 2019, 4, 1095−1102

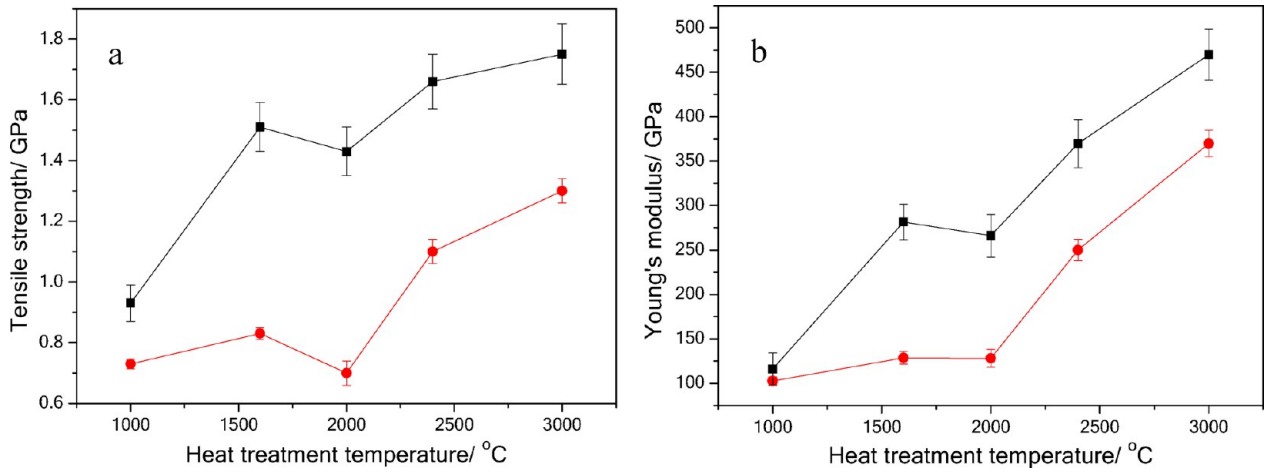

Figure 9. (a) Tensile strength and (b) Young's modulus of carbon fibers derived from the unstirred (black square) and stirred (red dot) pitches after heat treatment at various temperatures.

2.4. Physical Properties of the Derivative Carbon Fibers. The tensile strength and Young's modulus of the two types of fibers after heat treatment at various temperatures are shown in Figure 9. It can be clearly seen from the graphs shown in Figure 9a, b that the tensile strength and Young's modulus of the carbon and graphite fibers prepared from the unstirred pitch are much higher than those of the fibers derived from the stirred pitch as a result of the orientation, size, and stacking of the graphene layers within the graphite fibers as shown in their fracture surfaces (Figure 10). The microcrystal

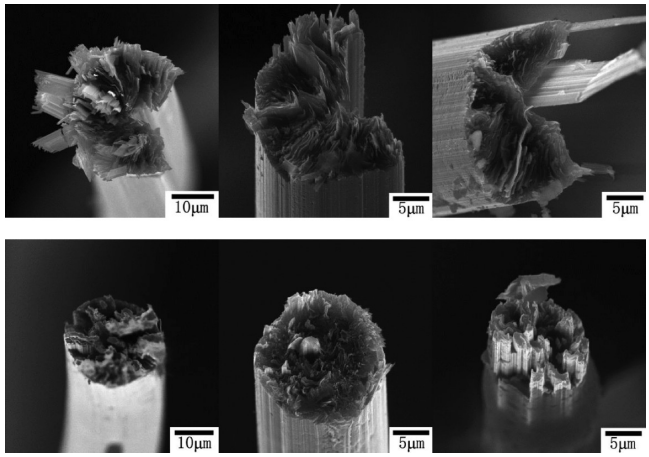

Figure 10. Typical SEM images of cross sections of single carbon fibers derived from the unstirred (top row) and stirred (bottom row) pitches after heat treatment at 3000 °C showing the microstructure of their fracture surfaces after tensile testing.

size, stacking thickness of graphene layers, and degree of preferred orientation of the 3000 °C-graphitized fibers derived from the unstirred pitch are markedly greater than those of the fibers derived from the stirred pitches, resulting in an anticipated significant increases in the mechanical property, which is in agreement with previous studies. However, the dispersion and standard deviation values of tensile strength and modulus of the carbon and graphite fibers derived from the unstirred pitch are obviously larger than those of fibers obtained from the stirred pitch, which may be closely associated with the "Pac-man" splitting texture and micro-structural disintegration of the former. The deviation of the cracking direction or inhomogeneous cracks in the fiber axis will cause a significant drop in the mechanical properties of the carbon fibers; some may be catastrophic. It is interesting to note that the tensile strength and Young's modulus of the 3000 °C-graphitized large fibers with a radial-folded texture (shown in Figure 6) are measured to be as high as 1.6 and 420 GPa. It can be observed that the tensile property of graphite fibers is mostly dominated by the orientation and size of graphite crystallites as clearly shown in the fracture sections and lattice fringe images. In comparison with commercial mesophase pitch-based carbon fibers with a small diameter of ~10 μm, the mechanical properties of large-diameter carbon fibers (strength: 1.3−1.8 GPa, modulus: 350−500 GPa) seem to be unsatisfactory,[2] but their axial electrical and thermal conduction properties are promising.[28] As the heat treatment progresses, the mechanical properties of these large fibers firstly increase, then decrease, and finally increase again. It is unexpected that the mechanical properties of these large fibers drop significantly upon heat treatment around 2000 °C. This may be due to the significant intrinsic structural development and evolution (e.g., crystalline orientation/size change and nanoscale flaws) taking place within the large-diameter fibers at this temperature.[1,29]

Figure 11 plots the axial electrical resistivity values of the carbon fibers derived from the unstirred and stirred pitches after heat treatment at various temperatures. The error bars are not provided in the graph owing to the relative low standard deviation (less than 5%) of both samples. The axial electrical resistivities of both types of fiber significantly decrease with the increase of HTT from 1000 to 3000 °C. There is no obvious difference in the axial electrical resistivities for the two types of 1000 °C-carbonized fibers. Upon further heat treatment of the carbon fiber samples up to the graphitization temperature, the axial electrical resistivities of the two kinds of large fibers show obvious differences; the graphite fibers derived from the unstirred pitch possess a lower axial electrical resistivity in comparison with that of graphite fibers derived from the stirred pitch, which is closely associated with the near-perfect crystal structure in the former as demonstrated above. The axial room-temperature electrical resistivities of the 3000 °C-graphitized fibers derived from the unstirred and stirred pitches were measured to be as low as 1.18 and 1.86 $\mu\Omega$ m,

DOI: 10.1021/acsomega.8b03189
ACS Omega 2019, 4, 1095−1102

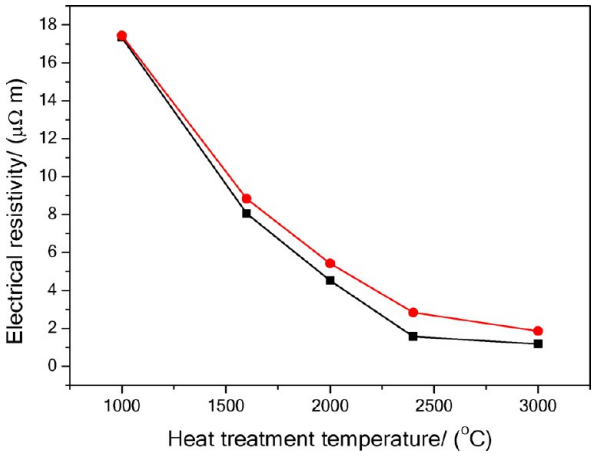

Figure 11. Room-temperature axial electrical resistivities of carbon fibers derived from the unstirred (black square) and stirred (red dot) pitches after heat treatment at various temperatures.

respectively. According to Lavin's thermal−electrical correlation,[30] the axial room-temperature thermal conductivities of these two types of large graphite fibers are about 875 and 695 W m^{-1} K^{-1}, respectively. These values are much higher than those of metallic thermal conduction materials (e.g., Cu and Al). The thermal conduction property is also closely related with the crystalline size and preferred orientation of the carbon fibers, which is highly consistent with the previous research results.[22,31]

3. CONCLUSIONS

This work clearly demonstrates the effects of a liquid crystalline mesophase texture in the pitch melts on the microstructure and physical properties of the resulting large-diameter carbon and graphite fibers. Thermomechanical stirring on the bulk mesophase pitch with high liquid crystalline orientation is a simple and effective method to adjust the structure and properties of mesophase-pitch-derived carbon fibers for various applications (or choose a randomly oriented liquid crystalline mesophase pitch as the precursor to directly prepare the desired carbon fibers). In this system, the tensile strength, modulus, axial electrical resistivity, and calculated thermal conductivity of the 3000 °C-graphitized fibers with a large diameter of ∼22 μm can be tuned to around 1.3−1.8 GPa, 350−500 GPa, 1.1−1.9 $\mu\Omega$ m, and 700−880 W m^{-1} K^{-1}, respectively, by modifying the liquid crystalline mesophase texture of the pitch precursors. The rheological structure of the molten pitch precursor strongly dictates the microstructure (crystallite size and preferred orientation) of the resulting carbon fibers, which in turn strongly influences the fibers' final physical properties. Carbon fibers derived from the stirred pitch possess smaller crystallite sizes, lower crystallite orientation, and inferior mechanical and transport properties in comparison with carbon fibers derived from the unstirred pitch. However, they can maintain their circular transverse cross section and prevent "Pac-man" splitting during heat treatment processes, which is beneficial to the microstructural homogeneity and mechanical stability (i.e., low strength deviation and dispersion). This characteristic will undoubtedly promote the wide application of pitch-based carbon fibers in composites.

4. EXPERIMENTAL SECTION

4.1. Materials. A commercial naphthalene-derived synthetic mesophase pitch (AR-MP, black pellet) was purchased from Mitsubishi Gas Chemical Corp. This type of mesophase pitch has a 100% optically anisotropic content and highly oriented liquid crystalline texture. Its softening point is 265 °C, measured on a hot stage with flowing nitrogen under a Carl Zeiss AX10 polarized light microscope (PLM). The raw pitch was heated in a stainless autoclave to about 320 °C and then vigorously stirred for 4 h with an agitating speed of ∼800 rpm to obtain the melt-stirred mesophase pitch with a chaotic liquid crystalline texture. The softening point of the melt-stirred pitch increased slightly to 273 °C. The as-received (unstirred) and melt-stirred mesophase pitches were both used as raw materials for the spinning of large-diameter pitch fibers.

4.2. Preparation and Heat Treatment of Large-Diameter Pitch Fibers. A uniformly molten mesophase pitch preheated in a stainless vessel was extruded under a nitrogen pressure of ∼0.2 MPa through a cylindrical die with a diameter of about 300 μm at a spinning temperature of 320−330 °C to form large-diameter pitch fibers (Φ, ∼30 μm), which were drawn and collected by winding onto a rotating drum at a rotational speed of ∼20 m/min.

The as-spun pitch fibers, stacked into a thin layer on a graphite plate, were stabilized at ∼240 °C for ∼30 h in a flowing oxygen atmosphere with a flow rate of 300 mL/min. After complete stabilization treatment, the stabilized pitch fibers were subsequently carbonized at 1000 °C (and 1600 °C) for 1 h under a nitrogen atmosphere in a tube furnace using a heating rate of 1 °C/min. The 1000 °C-carbonized fibers were finally graphitized at 2000, 2400, and 3000 °C at a heating rate of 12−15 °C/min for 30 min in a medium-frequency induction furnace under a flow of argon to obtain various graphite fibers.[18]

4.3. Characterization of the Pitch and Carbon Fibers. Mesophase pitch feedstock and its derivative carbon fibers (including coke) were embedded in a block of polyester resin and then carefully polished with fine sand paper. The surfaces of the pitches, coke, and cross sections of the fibers were then observed under a PLM in reflectance mode. The morphology and microstructure of the carbon and graphite fibers having undergone various high-temperature heat treatments were imaged with a TESCAN VEGA 3 scanning electron microscope (SEM).

The microcrystalline parameters of various fiber samples in their powder form were determined by X-ray diffraction (XRD) analysis using Cu K_α radiation (λ = 0.15406 nm). Raman spectra of the carbon and graphite fibers in their powder form were collected using a Renishaw InVia 2000 Raman microscope using 514.5 nm Ar^+ radiation for excitation at a power of 25 mW.

The tensile properties of the carbonized and graphitized fibers, treated at various temperatures from 1000 to 3000 °C, were measured by single-filament testing according to ASTM standard D3822-07 at a gauge length of 20 mm. About 30−40 fibers of each sample were tested; the average value of the measured data with an error of less than 10% was adopted, and the standard deviation of tensile strength was recorded. The broken fiber ends were saved for transverse area measurements and fracture surface analyses using SEM.

The axial electrical resistivities of the carbon fibers, heat-treated at various temperatures, were obtained by measure-

DOI: 10.1021/acsomega.8b03189
ACS Omega 2019, 4, 1095−1102

ment averaging of 15−20 individual carbon fibers with a BS407 precision milli/micro-ohmmeter using a standard four-probe method at room temperature. The axial room-temperature thermal conductivities of the various carbon fibers were calculated according to the accepted formula reported by Lavin.[30]

AUTHOR INFORMATION

Corresponding Authors

*E-mail: yuanguanming@wust.edu.cn (G.Y.).
*E-mail: xkli@21cn.com (X.L.).

ORCID

Guanming Yuan: 0000-0002-4693-8358

Notes

The authors declare no competing financial interest.

ACKNOWLEDGMENTS

This work was sponsored by the National Natural Science Foundation of China (grant No. 51372177) and the Key Laboratory of Hubei Province for Coal Conversion and New Carbon Materials (grant No. WKDM201701). The authors sincerely thank Wancai Peng for mechanical measurements of carbon fibers.

REFERENCES

(1) Frank, E.; Ingildeev, D.; Steudle, L. M.; Spörl, J. M.; Buchmeiser, M. R. Carbon fibers: precursor systems, processing, structure and properties. *Angew. Chem. Int. Ed.* **2014**, *53*, 5262−5298.

(2) Minus, M. L.; Kumar, S. The processing, properties, and structure of carbon fibers. *JOM* **2005**, *57*, 52−58.

(3) Emmerich, F. G. Young's modulus, thermal conductivity, electrical resistivity and coefficient of thermal expansion of mesophase pitch-based carbons fibers. *Carbon* **2014**, *68*, 274−293.

(4) Hurt, R. H.; Chen, Z. Y. Liquid crystals and carbon materials. *Phys. Today* **2000**, *53*, 39−44.

(5) Edie, D. D. The effect of processing on the structure and properties of carbon fibers. *Carbon* **1998**, *36*, 345−362.

(6) Korai, Y.; Hong, S. H.; Mochida, I. Meso-scale texture of mesophase pitch and its spun fiber. *Carbon* **1998**, *36*, 79−85.

(7) Mochida, I.; Yoon, S. H.; Takano, N.; Fortin, F.; Korai, Y.; Yokogawa, K. Microstructure of mesophase pitch-based carbon fiber and its control. *Carbon* **1996**, *34*, 941−956.

(8) Lafdi, K.; Bonnamy, S.; Oberlin, A. Mechanism of formation of the texture and microtexture in as-spun then oxidized anisotropic pitch-based carbon fibers, part I: radial with wedge type I1. *Carbon* **1992**, *30*, 551−567.

(9) Yoon, S. H.; Takano, N.; Korai, Y.; Mochida, I. Crack formation in mesophase pitch-based carbon fibres: Part I some influential factors for crack formation. *J. Mater. Sci.* **1997**, *32*, 2753−2758.

(10) Yoon, S. H.; Korai, Y.; Mochida, I. Crack formation in mesophase pitch-based carbon fibres: Part II detailed structure of pitch-based carbon fibres with some types of open cracks. *J. Mater. Sci.* **1997**, *32*, 2759−2769.

(11) Hamada, T.; Nishida, T.; Furuyama, M.; Tomioka, T. Transverse structure of pitch fiber from coal tar mesophase pitch. *Carbon* **1988**, *26*, 837−841.

(12) Mochida, I.; Yoon, S. H.; Korai, Y. Control of transversal texture in circular mesophase pitch-based carbon fibre using non-circular spinning nozzles. *J. Mater. Sci.* **1993**, *28*, 2331−2336.

(13) Matsumoto, M.; Iwashita, T.; Arai, Y.; Tomioka, T. Effect of spinning conditions on structures of pitch-based carbon fiber. *Carbon* **1993**, *31*, 715−720.

(14) Yao, Y.; Chen, J.; Liu, L.; Dong, Y.; Liu, A. Tailoring structures and properties of mesophase pitch-based carbon fibers based on isotropic/mesophase incompatible blends. *J. Mater. Sci.* **2012**, *47*, 5509−5516.

(15) Yao, Y.; Chen, J.; Liu, L.; Dong, Y.; Liu, A. Mesophase pitch-based carbon fiber spinning through a filter assembly and the microstructure evolution mechanism. *J. Mater. Sci.* **2014**, *49*, 191−198.

(16) Cho, T.; Lee, Y. S.; Rao, R.; Rao, A. M.; Edie, D. D.; Ogale, A. A. Structure of carbon fiber obtained from nanotube-reinforced mesophase pitch. *Carbon* **2003**, *41*, 1419−1424.

(17) Alway-Cooper, R. M.; Anderson, D. P.; Ogale, A. A. Carbon black modification of mesophase pitch-based carbon fibers. *Carbon* **2013**, *59*, 40−48.

(18) Yuan, G.; Li, X.; Xiong, X.; Dong, Z.; Westwood, A.; Li, B.; Ye, C.; Ma, G.; Cui, Z.; Cong, Y.; Zhang, J.; Li, Y. A comprehensive study on the oxidative stabilization of mesophase pitch-based tape-shaped thick fibers with oxygen. *Carbon* **2017**, *115*, 59−76.

(19) Cato, A. D.; Edie, D. D. Flow behavior of mesophase pitch. *Carbon* **2003**, *41*, 1411−1417.

(20) Kundu, S.; Ogale, A. A. Rheostructural studies on a synthetic mesophase pitch during transient shear flow. *Carbon* **2006**, *44*, 2224−2235.

(21) Blanco, C.; Appleyard, S. P.; Rand, B. Study of carbon fibres and carbon−carbon composites by scanning thermal microscopy. *J. Microsc.* **2002**, *205*, 21−32.

(22) Yuan, G.; Li, X.; Yi, J.; Dong, Z.; Westwood, A.; Li, B.; Cui, Z.; Cong, Y.; Zhang, J.; Li, Y. Mesophase pitch-based graphite fiber-reinforced acrylonitrile butadiene styrene resin composites with high thermal conductivity. *Carbon* **2015**, *95*, 1007−1019.

(23) Jeon, Y. P.; Cooper, R. A.; Morales, M.; Ogale, A. A. Carbon fibers. In *Handbook of Advanced Ceramics-materials, Applications, Processing and Properties*; Somiya, S., Eds.; Elsevier Science Ltd., 2013; pp 143-154. DOI: DOI: 10.1016/B978-0-12-385469-8.00009-5.

(24) Kundu, S.; Ogale, A. A. Rheostructural studies of a discotic mesophase pitch at processing flow conditions. *Rheol. Acta.* **2010**, *49*, 845−854.

(25) Iwashita, N.; Park, C. R.; Fujimoto, H.; Shiraishi, M.; Inagaki, M. Specification for a standard procedure of X-ray diffraction measurements on carbon materials. *Carbon* **2004**, *42*, 701−714.

(26) Maire, J.; Mering, J. Graphitization of soft carbons. In *Chemistry and Physics of Carbon*; Walker, P. L., Eds.; Marcel Dekker Inc., New York, 1970; pp 125-190. DOI: DOI: 10.1016/0008-6223(71)90037-6.

(27) Tuinstra, F.; Koenig, J. L. Raman spectrum of graphite. *J. Chem. Phys.* **1970**, *53*, 1126−1130.

(28) Lu, S.; Blanco, C.; Rand, B. Large diameter carbon fibres from mesophase pitch. *Carbon* **2002**, *40*, 2109−2116.

(29) Oberlin, A. Carbonization and graphitization. *Carbon* **1984**, *22*, 521−541.

(30) Lavin, J. G.; Boyington, D. R.; Lahijani, J.; Nystem, B.; Issi, J. P. The correlation of thermal conductivity with electrical resistivity in mesophase pitch-based carbon fiber. *Carbon* **1993**, *31*, 1001−1002.

(31) Gallego, N. C.; Edie, D. D. Structure-property relationships for high thermal conductivity carbon fibers. *Compos. Part A* **2001**, *32*, 1031−1038.

DOI: 10.1021/acsomega.8b03189
ACS Omega 2019, 4, 1095−1102